Clin Exp Metastasis (2008) 25:517–529
DOI 10.1007/s10585-008-9163-5

RESEARCH PAPER

A highly bone marrow metastatic murine breast cancer model established through in vivo selection exhibits enhanced anchorage-independent growth and cell migration mediated by ICAM-1

Munehisa Takahashi · Mutsuo Furihata · Nobuyoshi Akimitsu · Morihiro Watanabe · Sunil Kaul · Noboru Yumoto · Tomoko Okada

Received: 29 June 2007 / Accepted: 3 March 2008 / Published online: 14 March 2008
© Springer Science+Business Media B.V. 2008

Abstract To understand the mechanisms underlying bone marrow metastasis precisely, we established the highly metastatic 4T1E/M3 murine breast cancer cell line. 4T1 murine breast cancer cells were transfected with the neomycin resistance gene, selected in G418, intravenously injected into mice, and harvested from bone marrow. By repeating this protocol three times, we established the 4T1E/M3 cells. The clonality of 4T1E/M3 cells was markedly high confirmed by genomic southern analysis using neo-gene probe. When tissues harvested from mice after intravenous injection of 4T1E/M3 cells were examined histologically, markedly enhanced bone marrow metastasis was observed; 77% of spines from 4T1E/M3-injected mouse showed metastasis as compared to 14% metastasis seen with the parent cells. In vitro, 4T1E/M3 cells attached more strongly to the plastic plate and to bone marrow-derived endothelial cells. DNA micro arrays, real time RT-PCR and FACS analyses revealed that the expression of ICAM-1 and $\beta 2$ integrin was upregulated in 4T1E/M3 cells at both the mRNA and cell surface protein levels. 4T1E/M3 cells also showed greater anchorage-independent proliferation in soft agar, and migrated markedly faster than the parent cells in wound healing assays. Anti-ICAM-1 antibodies strongly inhibited both the colony formation and the migration activity of 4T1E/M3 suggesting the importance of the role of ICAM-1. Our newly established highly metastatic 4T1E/M3 cells may provide a potentially powerful tool to study the molecular mechanisms of bone marrow metastasis and to identify new molecular targets for therapeutic interventions.

Keywords Breast cancer · Metastasis · Bone marrow · Anchorage-independent growth · Migration · ICAM-1

M. Takahashi · N. Akimitsu · T. Okada (✉)
Institute for Biological Resources and Functions, National Institute of Advanced Industrial Science and Technology (AIST), 1-1-1, Higashi, Tsukuba, Ibaraki 305-8566, Japan
e-mail: t.okada@aist.go.jp

M. Furihata
Department of Pathology, Kochi Medical School, Nankoku, Kochi 783-8505, Japan

M. Watanabe
Laboratory of Experimental Immunology, National Cancer Institute at Frederick, Building 560, Room 31-16A, Frederick, MD 21702-1201, USA

S. Kaul
Research Institute for Cell Engineering, National Institute of Advanced Industrial Science and Technology (AIST), 1-1-1, Higashi, Tsukuba, Ibaraki 305-8562, Japan

N. Yumoto
National Institute of Advanced Industrial Science and Technology (AIST), 1-1-1, Umezono, Tsukuba, Ibaraki 305-8568, Japan

Introduction

Distant organ metastasis is the primary cause of morbidity and mortality among cancer patients. Moreover, bone is one of the most common sites of metastasis [1], and more than 80% of breast cancer patients experience bone metastasis [2]. But despite the obvious importance of understanding the mechanisms involved in the process of bone metastasis, so far only a few bone marrow metastasis models have been developed. MDA-MB-231 is a widely used human breast carcinoma cell line. Intracardiac injection of these cells into nude mice represents a typical model used to study the mechanisms involved in the development of bone metastasis [3–7]. A similar model

involves intracardiac injection of TMD-231 cells, which were derived from the MDA-MB-231 line [8]. However, it is difficult to make intracardiac injections into mice. In addition, it is necessary to use immunodeficient animals to establish a human carcinoma in mice; consequently, it is difficult to assess the role of the interaction of tumor cells with host cells in these animals. Nonetheless, the importance of the microenvironment of the tumor-host interface during the process of tumor progression and metastasis [9] has been illustrated. For instance, it was recently reported that tumor-associated macrophages facilitate angiogenesis and extracellular matrix breakdown and support tumor cells in their microenvironment [10, 11].

To overcome the disadvantages of using of immunodeficient mice, we have endeavored to establish a murine syngenic tumor model that is highly metastatic to bone marrow. To-date, there are only a few murine tumor models that show bone marrow metastasis. BALB/c-derived 4T1 spontaneous mouse mammary carcinoma cell line [12] was shown to closely mimic human breast cancer with respect to its immunogenicity, metastatic properties and growth characteristics [13, 14]. These cells have been used to develop a number of immunotherapies [15–17]. We, therefore, decided to use 4T1 cells to establish its bone marrow metastatic variant. By the characterization of the highly metastatic variant (4T1E/M3), we found that (i) these cells have higher anchorage independent growth and migration activity than the parent cells and (ii) Intercellular Adhesion Molecule-1 (ICAM-1) plays an important role in these activities. We anticipate that this new, highly metastatic 4T1E/M3 cells will be a useful model with which to study the mechanisms underlying bone marrow metastasis and to identify new molecular targets for therapeutic interventions.

Material and methods

Animals

Six to seven week-old female BALB/c mice were purchased from Japan Clea (Tokyo, Japan) or SLC (Shizuoka, Japan).

Cells

BALB/c-derived 4T1 (CRL-2539) mouse mammary carcinoma cells were obtained from the American Type Culture Collection (ATCC, Manassas, VA). The tumor growth and metastatic spread of 4T1 cells in BALB/c mice closely resembles human breast cancer, and these cells are considered an animal model for stage IV human breast cancer [13, 14]. 4T1 cells were cultured at 37°C under 5% CO_2 in RPMI 1640 medium containing 2 mM L-glutamine, adjusted to contain 1.5 g/l sodium bicarbonate, 4.5 g/l glucose, 10 mM HEPES, 1.0 mM sodium pyruvate, 10% fetal calf serum (Cancera International Inc. Ontario, Canada).

Establishment of the 4T1E/M3 cell line

4T1 cells were initially transfected with the neomycin resistance gene (Neo-gene; in pEGFP-F vector; BD Biosciences Clontech, Palo Alto, CA) using Effecten (QIAGEN, Valencia, CA), after which the transfectants were selected by culture in G418 (Geneticin, 120 μg/ml, Invitrogen) supplemented medium. After the death of any untransfected original 4T1 cells, the remaining G418-resistant cells were defined as parent cells. Parent cells (1×10^6/mouse) were then intravenously injected into BALB/c mice. Twelve days later the mice were sacrificed, and the femora and tibiae were harvested and flushed with culture medium using a 25 G needle and syringe (Terumo Co. Ltd., Tokyo, Japan), and the cells obtained were cultured in the medium containing G418 (120 μg/ml). After about 10 days, colonies of adherent cells began to emerge in the cultures. By contrast, no cells appeared in cultures of bone marrow from mice injected with original 4T1 cells. The growing cells were then intravenously injected into a new set of mice, and this cycle was repeated three times to establish the 4T1E/M3 cell line. Thereafter, 4T1E/M3 cells were maintained in the medium containing G418 (120 μg/ml). The cells harvested after the first and second selection in vivo were named as 4T1E/M1 and 4T1E/M2, respectively.

Genomic southern analysis of parent, 4T1E/M1, -M2, and -M3

Subconfluent monolayers of parent, 4T1E/M1, -M2, or -M3 cells in 15-cm dishes were washed by PBS three times, scraped by cell scraper (BD Bioscience), collected and then centrifuged. After removing the supernatant, the cell pellets were frozen at −80°C. Genomic DNAs were extracted from these pellets by lysis solution (50 mM Tris-HCl pH = 8.0, 100 mM NaCl, 1% SDS, 20 mM EDTA and 1 mg/ml protenase K) and purified in EtOH. Resuspended genomic DNAs in H_2O_2 were digested by *Eco*RI, *Hind*III, *Eco*O109I or *Bam*HI (50 units in 100 μl for each enzyme, Takara Biotechnology Ltd. Osaka, Japan) at 37°C for 12 h and then separated by electrophoresis on 0.8% agarose gel [18]. Transferred DNAs on nylon membrane (Immobilon NY+, Millipore Co. Billerica, MA) were hybridized with ^{32}P-labeled neo-gene probe, a 1.3 Kb *Stu*I-*Eco*O109I fragment coding neomycin-resistance gene derived from pEGPF-N1 (GenBank Accession #U55762) and visualized by image analyzer, BAS2500 (Fuji film, Tokyo, Japan).

In vivo tumor experiment

To analyze the experimental metastasis, parent or 4T1E/M3 cells (5×10^5/mouse) were initially injected into the tail vein of mice ($n = 10$) whose survival was then monitored. Animals were sacrificed when they became moribund. To assess metastasis, mice ($n = 21$ or 22) were intravenously injected with parent or 4T1E/M3 cells (1×10^6/mouse); 10 days later the mice were sacrificed, and the lung, liver, spleen, kidney, heart, and bone marrow (femur, tibia and spine) were harvested, and their histological sections were examined.

For analysis of spontaneous metastasis, parent or 4T1E/M3 cells (2×10^5/mouse) were subcutaneously injected into the backs of mice ($n = 10$), and their survival was monitored. Animals were sacrificed when they became moribund. To assess metastasis, mice ($n = 10$) were subcutaneously injected with parent or 4T1E/M3 cells (2×10^5/mouse); 30 days later the mice were sacrificed, and the lung, liver, spleen, kidney, heart, and bone marrow (femur, tibia and spine) were harvested and their histological sections were examined. Each experiment was repeated by three times.

All animal studies were reviewed and approved by the Institutional Animal Care and Use Committee of National Institute of Advanced Industrial Science and Technology (AIST).

Histology

Sections of lung, liver, spleen, kidney, heart, femur, tibia and spine from mice were fixed in 10% neutral buffered formalin (Wako Pure Chemical Industries, Ltd. Osaka, Japan), processed, embedded in paraffin, sectioned at 5–6 μm, stained with H&E, examined, and photographed under the microscope. The femur, tibia and spine were decalcified by decalcifying solution A (Plank Rychlo Method, Wako Pure Chemical Industries) following the manufacture's protocol before embedding.

RNA isolation and quantitative RT-PCR

Total RNA was isolated from parent cells, 4T1E/M3 cells using an RNAeasy Midi Kit (QIAGEN, Valencia, CA) according to the manufacture's protocol. Using 1 μg samples of the total RNA, first strand cDNA was synthesized (First Strand cDNA Synthesis Kit for RT-PCR, Roche Diagnostics) in a 20 μl reaction volume using a PTC-200 peltier thermal cycler (Bio-Rad MJ Research). The RT protocol was 25°C for 10 min, 55°C for 30 min, 85°C for 5 min and 0°C for 5 min. Specific forward and reverse primers were designed using Primer 3 software (Genetyx Co., Tokyo) and synthesized by Fasmac Co. Ltd. (Kanagawa, Japan). The primer sequences (5′–3′) used were as follows: for GAPDH (glyceraldehyde-3-phosphate dehydrogenase, product size, 209 bp), ccc ctt cat tga cct caa cta c (forward) and tgg tgg tga aga cac cag tag a (reverse); for neomycin phosphotransferase (product size, 213 bp), ctt ttt gtc aag acc gac ctg t (forward) and agc cat gat gga tac ttt ctc g (reverse); for integrin β2 (product size, 201 bp), gca cca agt aca aag tca gca g (forward) and gtt ggt cga act cag gat tag c (reverse); and for ICAM-1 (product size, 194 bp), tca cca gga atg tgt acc tga c (forward) and ggc ttg tcc ctt gag ttt tat g (reverse). The PCR reactions were set up according to the Light Cycler manual (Roche Diagnostics). A master mixture of the reaction components was prepared using a Light Cycler Fast Start DNA Master SYBR Green I Kit (Roche Diagnostics). The PCR protocol entailed a denaturation step at 95°C for 8 min; 40 cycles of denaturation at 95°C for 10 s, annealing at 59°C for 10 s, and extension at 72°C for 12 s; and a final cooling step at 40°C for 30 s. For each reaction, the crossing point (defined as the cycle number at which the noise band intersects the fluorescent curves) was determined using the "Fit Point Method" in the Light Cycler software ver. 3.52 (Roche Diagnostics). Relative levels of mRNA were calculated using the software with a standard curve constructed using various concentrations of a 1:1 mixture of the RT product (parent and 4T1E/M3) and then normalized to level of GAPDH mRNA.

Proliferation assay

Parent or 4T1E/M3 cells (1×10^4/ml, 200 μl/well) were seeded into 96-well plates and cultured at 37°C under 5% CO_2. On the same day, or 1–4 days later, Cell Counting Kit-8 reagent (10 μl/well; Dojin, Tokyo, Japan) was added to wells, and the plates were incubated for an additional 4 h, after which the absorbance at 450 nm was measured using a microplate reader (model 680, Bio-Rad Laboratories, Inc., Hercules, CA). The Cell Counting Kit-8 assay [19] used is a modified MTT- assay [20].

Anchorage-independent proliferation assay

Anchorage-independent colony-formation in soft agar was assayed according to the previously published protocol [21, 22]. Briefly, parent or 4T1E/M3 cells (5×10^3/ml or 1×10^4/ml, 2 ml/dish) were seeded in 0.3% agarose (Difco noble agar, BD Diagnostic Systems, MD, USA) containing culture medium layered on 0.5% agarose medium (5 ml/dish) in 6-cm dishes and cultured at 37°C under 5% CO_2 for 12 days. To examine the effect of anti-ICAM-1 antibody, αICAM-1 (CD54, final concentration, 10 or 25 μg/ml, R&D Systems Inc. Minneapolis, MN), or control antibody (Rat IgG_{2B} Isotype Control, final concentration,

25 μg/ml, R&D Systems Inc.) were added in 0.3% agarose. Total numbers of colonies per dish were then counted, and the colonies formed were photographed under the microscope.

DNA microarray analysis

Total RNA was isolated from parent or 4T1E/M3 cells using an RNAeasy Midi Kit (QIAGEN) following the manufacture's protocol and then treated with the RNase-free DNase set (QIAGEN) to remove contaminating chromosomal DNA. Thereafter, 2 μg samples were used for microarray analysis performed by Takara Biotechnology Ltd. (Osaka, Japan) using a GeneChip mouse genome 430 2.0 array (Affimetrix Co., about 34,000 genes were analyzed).

Assay of adhesion to plastic plates

Parent or 4T1E/M3 cells (1×10^5/ml, 200 μl/well) were seeded into 96-well plates to form complete monolayers. The next day, the culture medium was removed, and phosphate-buffered saline containing 0.017% EDTA (EDTA-PBS; 200 μl/well) was added and incubated at 37°C for 5–60 min. The plates were then washed three times to remove detached cells, and culture medium was added (200 μl/well). Cell Counting Kit-8 reagent (10 μl/well; Dojin) was then added to the wells, followed by the incubation of the plates for an additional 4 h, after which the absorbance at 450 nm was measured using a microplate reader (model 680, Bio-Rad Laboratories, Inc.).

Assay of adhesion to endothelial cell monolayers

BMECs, bone marrow derived-endothelial cells [23] (1×10^5/ml, 1 ml/well) were seeded into 24-well plates and then incubated for 2–3 days, sufficient time for the cells to form complete monolayers. Parent or 4T1E/M3 cells (1×10^6/ml) were labeled with BCECF by incubation with membrane permeant BCECF-AM (5 μg/ml, Dojin, Tokyo, Japan) at 37°C for 30 min and then washed three times with the culture medium. The labeled cells were resuspended in culture medium (2×10^6/ml), after which the cells (100 μl/well) were seeded onto the confluent BMEC monolayers. The plates were then incubated at 37°C for 15–75 min and then washed three times to remove nonadherent cells. To examine the effect of anti-ICAM-1 (CD54; final concentration: 66 μg/ml, R&D Systems Inc. Minneapolis, MN) or anti-β2 integrin (CD18; final concentration: 66 μg/ml, BD Biosciences Pharmingen, San Jose, CA) were added to the BMEC monolayers before seeding the parent or 4T1E/M3 cells. The fluorescence was measured using a plate reader (Cyto FluorII, PerSeptive Biosystem, Ex: 485 nm, Em: 530 nm).

Flow cytometry

Parent cells, 4T1E/M3 cells or BMECs (1×10^6/200 μl in PBS containing 0.1% NaN_3 and 0.1% BSA) were incubated with monoclonal anti-ICAM-1 (CD54; final concentration: 5 μg/ml, R&D Systems Inc.) or anti-β2 integrin (CD18; final concentration: 5 μg/ml, BD Biosciences Pharmingen), on ice for 30 min. The cells were washed three times and then incubated with fluorescein isothiocyanate-conjugated F $(ab')_2$ goat anti-rat IgG (final concentration: 5 μg/ml, MP Biomedicals, Inc. Solon OH) on ice for 30 min. After three more wash, the cells were subjected to flow cytometric analysis (Epics Elite, Beckman-Coulter Inc. Fullerton, CA).

Wound healing assay

Parent or 4T1E/M3 cells (1×10^5/ml, 1 ml/well) were seeded into 24-well plates and incubated for 2 days. After confirming that a complete monolayer had formed, the monolayers were wounded by scratching lines with plastic tip. The wells were then washed once to remove any debris, observed and photographed under the microscope. To examine the effect of αICAM-1 antibodies (CD54, or isotype control, final concentration: 8 μg/ml, R&D System. Inc.) were added after the wash. Thereafter, the plates were incubated at 37°C under 5% CO_2 for 7.5 h, after which the cells were observed and photographed. The distance that the cells had migrated was measured on the photomicrographs [24]. The percent wounded area filled was calculated as follows: {(mean wounded breadth − mean remained breadth)/mean wounded breadth} × 100 (%)

Statistical analysis

Differences in mRNA expression and wound healing were analyzed using the Mann–Whitney *U* test. Mouse survival was evaluated by Kaplan–Meier analysis. Other data were statistically analyzed using one-way ANOVA followed by Bonferroni's multiple comparisons test. GraphPad Prism (Version 4; GraphPad Software, San Diego, CA, USA) was used for all statistical analyses.

Results

4T1E/M3 cells showed enhanced experimental bone marrow metastasis

To examine the in vivo metastatic activity of 4T1E/M3 cells, we initially intravenously injected parent or 4T1E/M3 cells into syngenic BALB/c mice and examined the survival rates. We found that mice injected with 4T1E/M3

cells died significantly earlier than those injected with parent cells (Fig. 1A), suggesting that in vivo the former were significantly more malignant than the latter. To assess the metastasis, we sacrificed mice 10 days after the cell injection for histological examination ($n = 22$ for 4T1E/M3 and $n = 21$ for parent cells) of their tissues (Table 1). We detected metastases in the spines (17/22: 77%), femur (1/22: 4.5%), lungs (22/22: 100%), livers (1/22: 4.5%), spleens (2/22: 9.1%) and heart (1/22: 4.5%) from 4T1E/M3-injected mice. Photographs of the metastasis in femur and spine from 4T1E/M3-injected mice were shown in Fig. 1B. On the other hand, metastases were detected in spines (3/21: 14%), lungs (21/21: 100%) and spleens (2/21: 9.5%) from parent cell-injected mice. No kidney or tibia metastasis was detected from any mice. It is notable that the frequency of spine metastasis was much higher in the 4T1E/M3 cell (77%) than the parent cells (14%).

4T1E/M3 cells showed enhanced spontaneous bone marrow metastasis

We, next, subcutaneously injected mice with parent or 4T1E/M3 cells ($n = 10$) in order to evaluate the spontaneous metastatic activity. In this case, we found there to be no significant difference in survival between parent cell- and 4T1E/M3-injected mice (Fig. 2). In another experiment, mice ($n = 10$) were subcutaneously injected with cells and then sacrificed 30 days later, after which histological analysis was carried out (Table 1). Metastases were detected in spines (2/10: 20%) form 4T1E/M3-injected mice, while they were not detected in spines (0/10: 0%) from parent cell-injected mice. We also found that 4T1E/M3 cells were more metastatic to lung (10/10: 100%) compared to parent cells (5/10: 50%).

Taken together, these findings indicate that the metastatic activity of the 4T1E/M3 cells, especially to spine, is

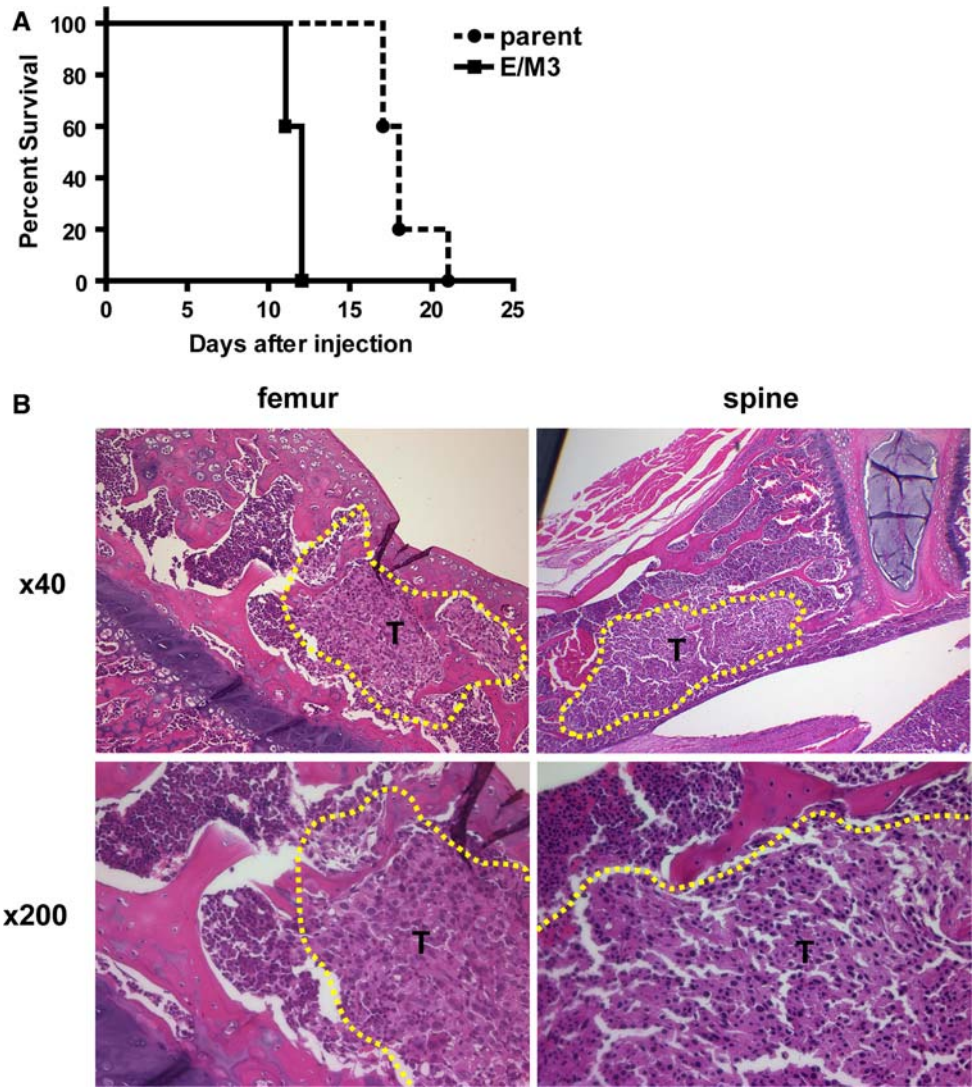

Fig. 1 Effects of intravenous injection of parent or 4T1E/M3 cells into mice. (**A**) Survival after injection of 5×10^5 cells/mouse ($n = 10$). (**B**) Histological detection of metastasis in tissue samples collected 10 days after injection of 1×10^6 cells/mouse. Metastasis in femur and spine were detected by H&E staining. The photomicrographs are shown at two magnifications: 40× and 200×. The 4T1E/M3 tumor (T) is indicated by a yellow dashed line

Table 1 Metastatic activity of 4T1E/M3 and parent cells

	Tissue							
	Spine	Femur[c]	Lung	Liver	Spleen	Kidney	Brain	Heart
Incidence of experimental metastasis[a]								
4T1E/M3	17/22 (77%)	1/22 (4.5%)	22/22 (100%)	1/22 (4.5%)	2/22 (9.1%)	0/22 (0%)	0/22 (0%)	1/22 (4.5%)
Parent	3/21 (14%)	0/21 (0%)	21/21 (100%)	0/21 (0%)	2/21 (9.5%)	0/21 (0%)	0/21 (0%)	0/21 (0%)
Incidence of spontaneous metastasis[b]								
4T1E/M3	2/10 (20%)	0/10 (0%)	10/10 (100%)	0/10 (0%)	0/10 (0%)	0/10 (0%)	0/10 (0%)	0/10 (0%)
Parent	0/10 (0%)	0/10 (0%)	5/10 (50%)	0/10 (0%)	0/10 (0%)	0/10 (0%)	0/10 (0%)	0/10 (0%)

[a] 1×10^6 cells/mouse were intravenously injected to mice and 10 days later the histological sections were examined

[b] 2×10^5 cells/mouse were subcutaneously injected to mice and 30 days later the histological sections were examined

[c] No metastasis to tibia was detected

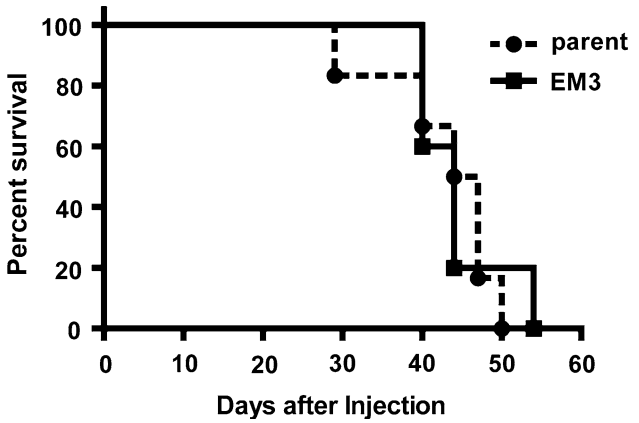

Fig. 2 Effects of subcutaneous injection of parent or 4T1E/M3 cells into mice. Survival after injection of 2×10^5 cells/mouse ($n = 10$) was analyzed

significantly augmented ($P < 0.001$), as compare to the parent cells, irrespective of whether the cells are administered intravenously or subcutaneously.

Clonality of 4T1E/M3 was remarkably high

To examine the clonality of 4T1E/M3, we performed the genomic southern analysis using the probe of neomycin resistance gene. As shown in Fig. 3, the transferred genomic DNAs, digested by indicated restriction enzyme, from parent cells formed a big smear but that from 4T1E/M3 showed a clear single band. Furthermore, single band was seen in spite of digestion by any of the enzymes examined (Fig. 3). The data suggests that although the 4T1E/M3 is a cell line, the clonality of the cells is markedly high. Interestingly, the DNAs from 4T1E/M1 and 4T1E/M2, the cells harvested after the first and second selection in vivo respectively, also gave a single band (Fig. 3). Taken together, the data suggest that the in vivo selection is quite useful to obtain the highly clonal cells in our model.

Proliferation of 4T1E/M3 cells was only slightly increased in vitro

To investigate the mechanism underlying the enhanced metastatic activity of 4T1E/M3 cells, we carried out a modified MTT assay to examine their in vitro proliferation rate. We found that 4T1E/M3 cells proliferated only slightly faster than parent cells (Fig. 4, significant for day 3 and 4, $P < 0.001$). Note that although 4T1E/M3 cells were usually cultured in medium containing G418 (120 μg/ml), their proliferation rate was unchanged when cultured for 4 days without G418.

Adhesion of 4T1E/M3 cells to plastic plates and to BMECs was significantly augmented

During the process of metastasis, it is very important for tumor cells to bind to elements in their microenvironment. To measure the capacity of the cells to bind to plastic plates, we first cultured parent or 4T1E/M3 cells to form monolayers on plastic 24-well plates. The monolayers were then incubated in EDTA-PBS for the indicated times and washed to remove any nonadherent cells. The numbers of remaining cells were then determined using modified MTT assays. Whereas parent cells readily detached from the plate in the presence of EDTA-PBS, 4T1E/M3 cells remained attached (Fig. 5A, $P < 0.001$ at 5, 10 and 20 min; $P < 0.01$ at 30 min). During the period from 5 to 20 min after addition of EDTA-PBS, about twice a many 4T1E/M3 cells as parent cells remained attached. Furthermore, we analyzed the adhesion activity of parent or 4T1E/M3 cells to bone marrow-derived endothelial cells, because the high binding activity to endothelial cells is also an important property for metastatic tumor cells. As a result, fluorescently labeled 4T1E/M3 cells also bound significantly more strongly than parent cells to BMEC monolayers (Fig. 5B, $P < 0.001$ at 30 min, $P < 0.01$ at 45 min, $P < 0.05$ at 15 and 75 min). Taken together,

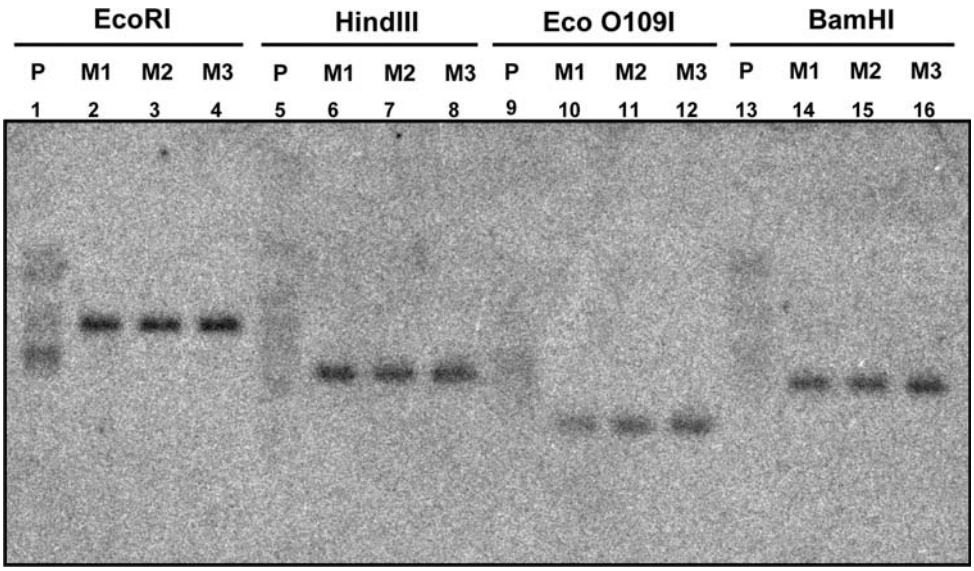

Fig. 3 Genomic southern analysis of parent, 4T1E/M1, -M2, and -M3. Genomic DNAs extracted from indicated cell lines (P: parent cell; M1:4T1E/M1 ; M2:4T1E/M2; M3:4T1E/M3) were digested with *Eco*RI (lanes 1–4), *Hind*III (lanes 5–8), *Eco*O109I (lanes 9–12) or *Bam*HI (lanes 13–16) and then separated by electrophoresis on 0.8% agarose gel, transferred to nylon membrane, and hybridized with ^{32}P-labeled neo-gene probe and visualized by image analyzer

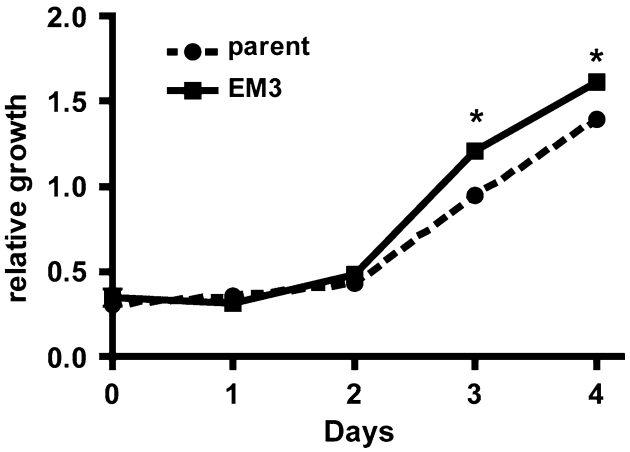

Fig. 4 In vitro proliferation activity of parent or 4T1E/M3 cells. Parent or 4T1E/M3 cells (2×10^3/well) were cultured in 96-well plates, after which cell numbers were determined using a modified MTT assay. * $P < 0.001$

4T1E/M3 cells showed stronger adhesion activity than parent cells both to plastic plate and bone marrow-derived endothelial cells.

Expression of β2 integrin and ICAM-1 was upregulated in 4T1E/M3 cells at both the mRNA and cell surface protein level

We, next, used a DNA micro-array to survey the differences in gene expression between 4T1E/M3 and parent cells with an aim of determining the genes involved in the increased adhesive activity of 4T1E/M3 cells. As shown in Table 2, among the genes related to cell adhesion, expression of ICAM-1 and β2 integrin was about 2–4 times higher in 4T1E/M3 cells than in parent cells in two independent experiments. This finding was confirmed by quantitative RT-PCR that showed the markedly higher level of expression of ICAM-1 or β2 integrin mRNA in 4T1E/M3 cells than parent cells (Fig. 6A, $P < 0.01$). Moreover, flow cytometric analysis showed that the cell surface expression of both β2 integrin and ICAM-1 was significantly higher on 4T1E/M3 cells than parent cells (Fig. 6B).

Anchorage-independent growth of 4T1E/M3 cells was remarkably accelerated and was suppressed by anti-ICAM-1 antibody

In contrast to normal adherent cells, tumor cells have the capability to grow without binding to a substrate; anchorage-independent proliferation is a hallmark of the malignancy of tumor cells. We, therefore, assessed the anchorage-independent proliferation of 4T1E/M3 and parent cells in soft agar colony formation assays. Twelve days after plating, both the parent and 4T1E/M3 cells in medium containing 0.3% agar showed the formation of colonies. As shown in Fig. 7A, however, 4T1E/M3 cells formed more than twice as many colonies as did parent cells. Moreover, the diameters of the 4T1E/M3 colonies were 2–3 times larger than those of the parent cell colonies (Fig. 7B).

Because the expression of ICAM-1 on 4T1E/M3 cells was remarkably augmented (Fig. 6B), we examined the effect of anti-ICAM-1 antibody on anchorage independent proliferation activity. The higher colony formation activity by 4T1E/M3 was strongly suppressed by anti-ICAM-1 antibody (Fig. 7A, $P < 0.01$), while the activity remained unchanged in the presence of the control antibody. We also confirmed that anti-ICAM-1 antibody did not affect the colony formation activity of parent cells (data not shown). The presence of anti-ICAM-1 antibody also decreased the size of the colonies of 4T1E/M3. Thus, 4T1E/M3 cells

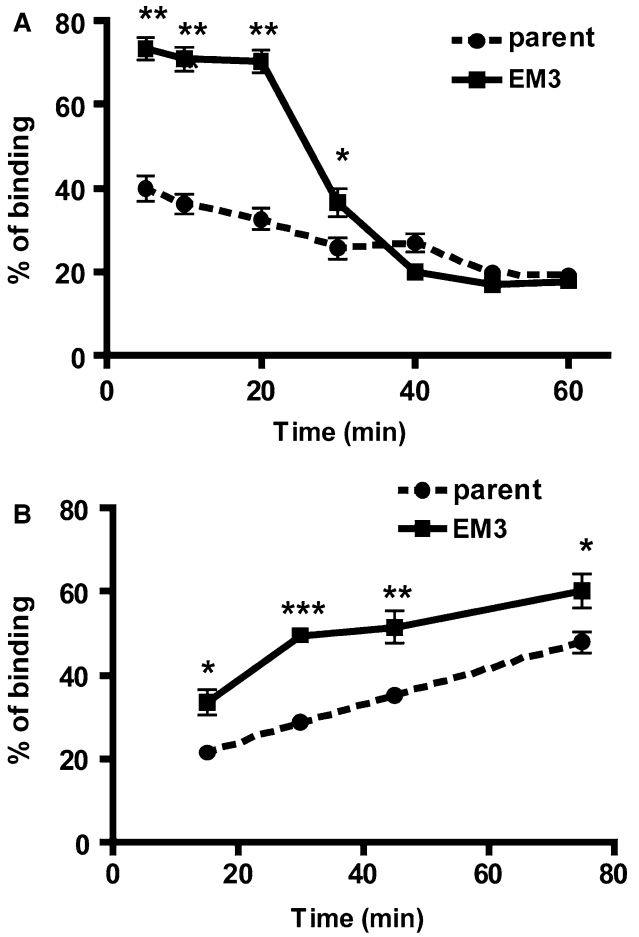

Fig. 5 In vitro adhesion activity of parent or 4T1E/M3 cells. (**A**) Adhesion to plastic plates. Parent or 4T1E/M3 cells (1×10^5/ml) were seeded into 96-well plates and cultured for 1 day, after which the medium was replaced with EDTA-PBS, and the plates were incubated for 5–60 min and washed. Numbers of adherent cells were determined using a modified MTT assay. Data are shown as means ± SD; ** $P < 0.001$; * $P < 0.01$. (**B**) Adhesion to BMECs. BCECF-AM-labeled parent or 4T1E/M3 cells (2×0^5/well) were placed on confluent monolayers of BMECs in 24-well plates, after which the plates were incubated for 15–75 min, washed, and the fluorescence was measured using a microplate reader. Data are shown as means ± SD; *** $P < 0.001$; ** $P < 0.01$; * $P < 0.05$

appear to have acquired a greatly enhanced capacity for anchorage-independent growth and the enhancement was mediated by ICAM-1.

Migration of 4T1E/M3 cells was also dramatically enhanced and was inhibited by anti-ICAM-1 antibody

The ability to migrate is another very important feature of metastatic tumor cells. We therefore carried out wound healing assays to analyze the migration of 4T1E/M3 and parent cells. Monolayers of parent or 4T1E/M3 cells in 24-well plates were wounded and then 7.5 h later the breadth of the wounds was measured. As shown in Fig. 8A, the wounds in the 4T1E/M3 monolayers recovered much more quickly than those in the parent cell monolayers. The percent area filled by 4T1E/M3 cells was about twice more larger than that filled by the parent cells (Fig. 8B, $P < 0.001$), and the wounds were completely healed after 24 h. We then analyzed the effect of anti-ICAM-1 antibodies on the migration of 4T1E/M3 cells. Just after the monolayers were wounded and washed, anti-ICAM-1 antibodies were added to the wells of 4T1E/M3. As a result, migration activity was strongly inhibited (Fig. 8B, $P < 0.001$). The data indicates that 4T1E/M3 cells have a greater ability to migrate than parent cells and the ICAM-1 molecules play some important role in the migration process.

Discussion

The 4T1 cell line is a thioguanine-resistant variant from a mammary tumor that arose spontaneously in a BALB/cfC_3H mouse without mutagen treatment [12]. 4T1 cells very closely mimic human breast cancer in its metastatic properties and growth characteristics [13]. In the present study, we established highly bone marrow metastatic variant from 4T1 cells by repeated in vivo selection. We found that, as compared to parent cells, 4T1E/M3 cells exhibited significantly greater metastatic activity when they were injected intravenously or subcutaneously into mice (Table 1). It is noteworthy that 4T1E/M3 cells exhibited a higher degree of metastatic activity especially to spine, where metastases are more frequently detected in breast cancer patients [25].

In the first round of establishment, cells extracted from femora and tibiae of mice grew well in culture. However, the parent cells did not show any metastasis in femur and tibia when examined in vivo (Table 1). The possibility of existence of low number of metastatic cells in the parent cells (that could not be detected by histological observation of tissues) cannot be ruled out.

The 4T1E/M3 cells also showed a high degree of lung metastasis. This is not surprising, as the original 4T1 cells also show considerable lung metastasis [13, 26]. We suggest this is an advantageous feature of our model, as clinically there are few tumors that metastasize solely to bone marrow. In other words, most tumors that metastasize to bone marrow also metastasize to other organs. Furthermore, in other models, investigators were required to make intracardiac injections to induce bone marrow metastasis [3–8, 27]. In our model, by contrast, we were able to successfully establish bone marrow metastasis through intravenous or subcutaneous injection. This means that the 4T1E/M3 cells potentially represent an easy to use and highly useful tumor model with which to investigate the mechanisms involved in bone marrow metastasis.

Table 2 Gene expressions corresponding to cell adhesion molecules between parent cells and 4T1E/M3 cells

Gene symbol[a]	GenBank	Experiment 1[b]	Log fold	Experiment 2[b]	Log fold
Cd44	AW146109	NC(P/P)	–	NC(P/P)	–
Cdh1	NM_009864	NC(P/P)	–	NC(P/P)	–
Cdh2	BC022107	NC(A/A)	–	NC(A/A)	–
Cdh3	X06340	NC(A/A)	–	NC(A/A)	–
Cdh4	NM_009867	NC(A/A)	–	NC(A/A)	–
Cdh5	NM_009868	NC(A/A)	–	NC(A/A)	–
Cdh6	NM_007666	NC(A/A)	–	NC(A/A)	–
Cdh7	BB129525	NC(A/P)	–	NC(A/A)	–
Cdh8	NM_007667	NC(A/A)	–	D(A/A)	−3.3
Cdh9	BQ176417	NC(A/A)	–	NC(A/A)	–
Cdh10	AK021064	NC(A/A)	–	NC(A/A)	–
Cdh11	NM_009866	NC(A/A)	–	NC(A/A)	–
Cdh13	AK016527	NC(A/A)	–	NC(A/A)	–
Cdh15	NM_007662	NC(A/A)	–	NC(A/A)	–
Cdh16	NM_007663	NC(A/A)	–	NC(A/A)	–
Cdh17	NM_019753	I(A/P)	1.2	NC(A/P)	–
Cdh20	NM_011800	NC(A/A)	–	NC(A/A)	–
Cdh22	AB019618	NC(A/M)	–	NC(A/P)	–
Cdh23	AK016015	NC(P/A)	–	NC(A/A)	–
Cdh26	BB748621	NC(A/A)	–	NC(A/A)	–
Icam1	BC008626	I(P/P)	1.5	I(P/P)	1.3
Icam2	NM_010494	NC(A/A)	–	NC(A/A)	–
Icam4	NM_023892	NC(A/A)	–	NC(A/A)	–
Icam5	NM_008319	NC(A/A)	–	NC(A/A)	–
Itga1	AV372589	NC(A/A)	–	NC(A/A)	–
Itga2	NM_008396	I(P/P)	1.4	NC(P/P)	–
Itga2b	NM_010575	NC(P/P)	–	NC(P/P)	–
Itga3	NM_013565	I(P/P)	0.3	NC(P/P)	–
Itga4	NM_010576	NC(A/A)	–	NC(A/A)	–
Itga5	BB493533	NC(P/P)	–	NC(M/P)	–
Itga6	BM935811	NC(P/P)	–	NC(P/P)	–
Itga7	NM_008398	NC(A/P)	–	D(P/A)	−0.6
Itga8	BB623587	NC(A/A)	–	NC(A/A)	–
Itga9	NM_133721	NC(A/A)	–	NC(A/A)	–
Itgae	NM_008399	NC(A/A)	–	NC(A/A)	–
Itgal	AF065902	NC(A/A)	–	NC(A/A)	–
Itgam	NM_008401	NC(A/A)	–	NC(A/A)	–
Itgav	NM_008402	D(P/P)	−0.6	NC(P/P)	–
Itgax	NM_021334	NC(A/A)	–	NC(A/A)	–
Itgb1	BM120341	NC(A/P)	–	NC(P/A)	–
Itgb2	NM_008404	I(P/P)	2.1	I(P/P)	1.8
Itgb2l	NM_008405	NC(A/A)	–	NC(A/A)	–
Itgb3	NM_016780	NC(A/A)	–	NC(A/A)	–
Itgb4	L04678	I(P/P)	2.3	NC(P/P)	–
Itgb5	NM_010580	I(P/P)	0.5	I(P/P)	0.3
Itgb6	NM_021359	NC(P/A)	–	NC(P/P)	–
Itgb7	NM_013566	NC(A/A)	–	NC(A/A)	–
Itgbl1	BC020152	NC(A/A)	–	NC(A/A)	–

Table 2 continued

Gene symbol[a]	GenBank	Experiment 1[b]	Log fold	Experiment 2[b]	Log fold
L1cam	NM_008478	I(P/P)	1.3	I(P/P)	1.1
Madcam1	BC024372	NC(M/P)	–	NC(A/A)	–
Pecam1	NM_008816	NC(A/A)	–	NC(A/A)	–
Vcam1	AV280637	NC(P/P)	–	NC(P/P)	–

Analyses were performed twice with independent mRNA preparations (experiments 1 and 2)

[a] Cd—Cluster of differentiation; Cdh—Cadherin; Icam—Intracellular adhesion molecule; Itga—Integrin alpha; Itgb—Integrin beta; L1cam—L1 cell adhesion molecule; Madcam—Mucosal addressin cellular adhesion molecule; Pecam—Platelet-endothelial cell adhesion molecule; Vcam—Vascular cell adhesion molecule

[b] NC—No change; D—Decrease (in 4T1E/M3); I—Increase (in 4T1E/M3); A—Absence; P—Presence; M—Marginal

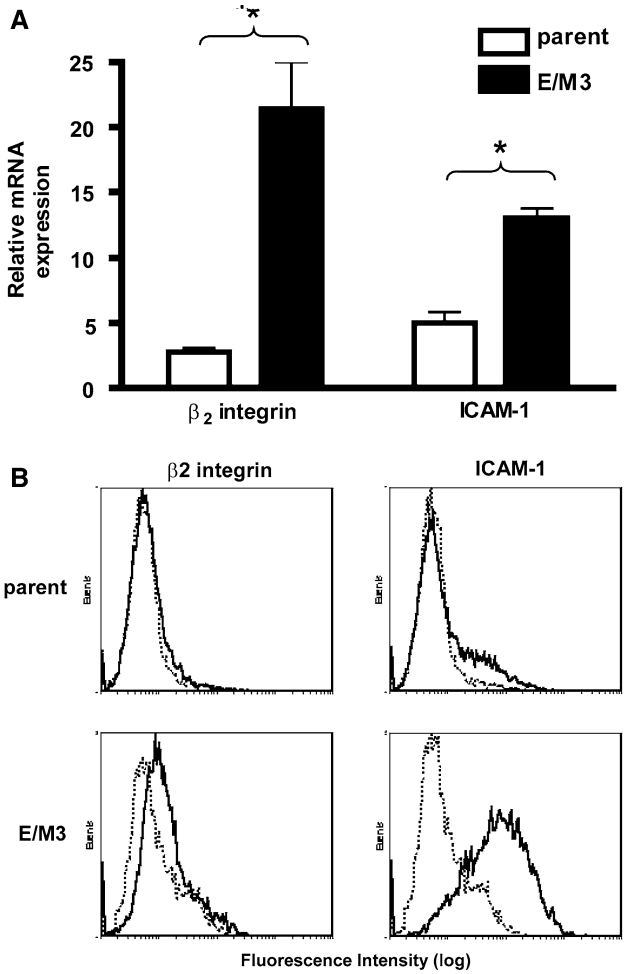

Fig. 6 Analysis of $\beta 2$ integrin and ICAM-1 expression. (**A**) mRNA expression. Expression of $\beta 2$ integrin and ICAM-1 mRNA in parent or 4T1E/M3 cells was analyzed by quantitative RT-PCR. Values are shown as Means ± SD; * $P < 0.01$. (**B**) Cell surface expression. Parent or 4T1E/M3 cells were stained by anti-$\beta 2$ integrin or anti-ICAM-1 antibody and subjected to flow cytometric analysis. Solid and dashed lines represent the experimental and control profiles, respectively

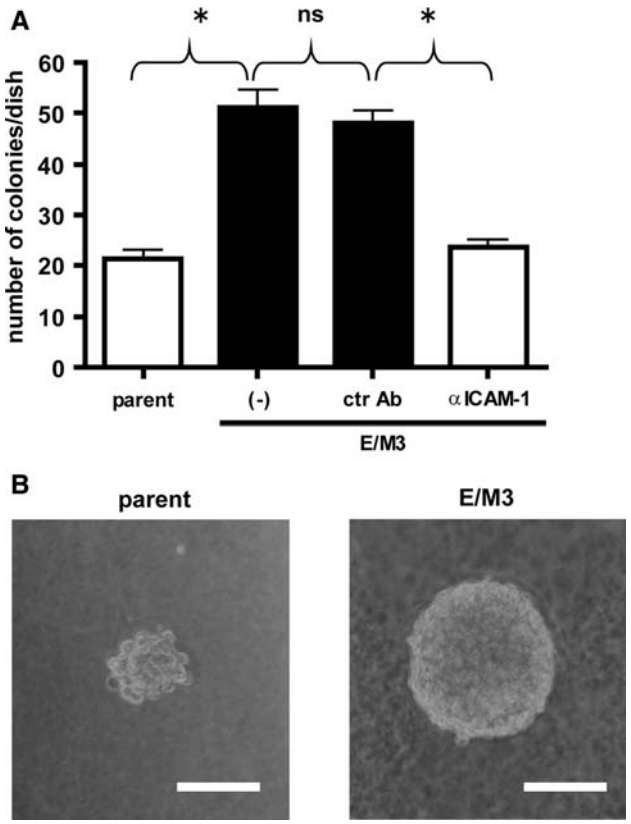

Fig. 7 In vitro anchorage-independent growth of parent or 4T1E/M3 cells. (**A**) Colony formation in soft agar. Parent or 4T1E/M3 cells (1×10^4/dish) were cultured for 12 days in medium containing 0.3% agarose with or without anti-ICAM-1 (25 μg/ml) or with isotype control antibody (25 μg/ml) layered on 0.5% agarose. Values shown are the average numbers of colonies per dish ± SD; * $P < 0.001$; ctr Ab, isotype control antibody. (**B**) Photomicrographs of the colonies (magnification, 100×). Scale bar: 100 μm

To analyze the clonality of 4T1E/M3, we performed the genomic southern analysis using the neo-probe. As shown in Fig. 3, it is apparent that the clonality of 4T1E/M3 is remarkably high. Moreover, both 4T1E/M1 and 4T1E/M2 cells harvested after the first and second in vivo selection, have high clonality. These results correspond to the reports of other earlier investigators [28, 29]. It is noteworthy that although 4T1E/M1, -M2 and -M3 originated from the same clone and possess the same genome, they show different level of malignancy and gene expression (data not shown).

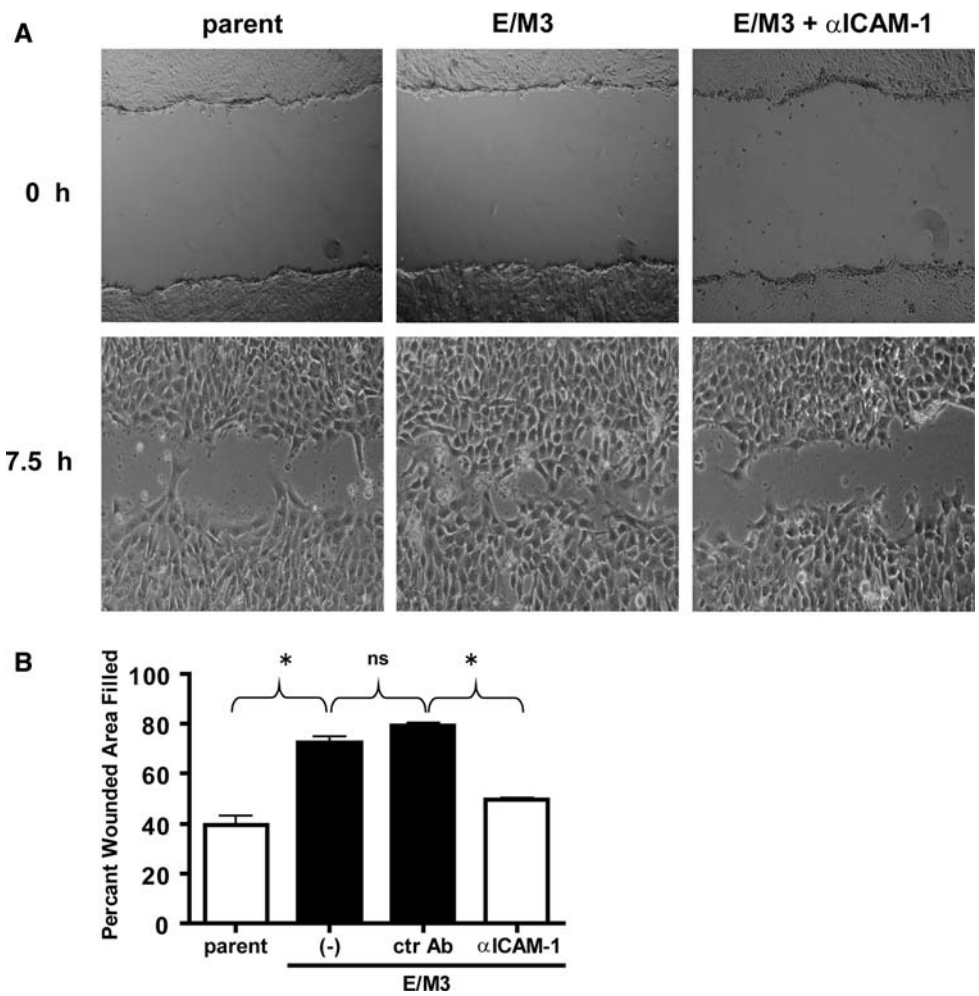

Fig. 8 In vitro migration activity of parent or 4T1E/M3 cells. (**A**) Confluent monolayers of parent or 4T1E/M3 cells in 24-well plates were wounded by scratching, after which the wells were washed, incubated with or without anti-ICAM-1 antibody (8 μg/ml) for 7.5 h and photographed. (**B**) Migration was assessed on the basis of percent wounded area filled in. Data are shown as means ± SD; * $P < 0.001$; ns, not significant; ctr Ab, isotype control antibody (8 μg/ml)

Thus, the in vivo selection could be a very significant way to obtain highly clonal and metastatic cells as seen in our model.

We found that the in vitro rate of 4T1E/M3 cell proliferation was slightly greater than that of parent cells, but the difference was not striking (Fig. 4). 4T1E/M3 cells also exhibited an increased capacity to adhere to plastic plates (Fig. 5A), which is consistent with an earlier report [30], and they also bound strongly to BMECs, bone marrow derived-endothelial cells (Fig. 5B). Expression of ICAM-1 and $\beta 2$ integrin was augmented in 4T1E/M3 cells at the levels of both the mRNA (Fig. 6A) and the cell surface protein (Fig. 6B). We expected that the BMECs used in the adhesion assay would express $\beta 2$ integrin (as a ligand to ICAM-1) or ICAM-1 (as a ligand to $\beta 2$ integrin), but somewhat surprisingly they did not express either. We added the anti-ICAM-1 or anti-$\beta 2$ integrin in the adhesion assay, but the antibodies showed no effect (data not shown). Consequently, it is not yet clear which adhesion molecules contribute to this stronger binding between 4T1E/M3 cells and BMECs.

Anchorage-independent proliferation is a hallmark of malignant cells that form tumors in vivo [31, 32] and is thought to be associated with highly metastatic cancer cells [33, 34]. For instance, a highly metastatic variant of mouse colon carcinoma established by repeated selection for liver metastasis in vivo showed enhanced colony formation activity [35]. The anchorage-independent growth of 4T1E/M3 cells in soft agar was similarly augmented (Fig. 7A). We suggest that this enhanced anchorage-independent proliferation is a key component of the enhanced metastatic activity of 4T1E/M3 cells.

We also found that cell migration, as assessed in wound healing assays (Fig. 8A, B), was dramatically augmented in 4T1E/M3 cells, as compared to parent cells. A strong capacity for migration is another hallmark of tumor malignancy [36]. In a number of studies, highly metastatic tumor cells exhibited upregulated migration in wound healing assays [37] and in in vitro invasion assays carried out using Boyden chambers [38, 39]. We therefore suggest that an augmented ability to migrate is another important feature underlying the enhanced metastatic activity of 4T1E/M3 cells.

Furthermore, anti-ICAM-1 antibodies strongly inhibited both the anchorage-independent proliferation (Fig. 7A) and

the migration (Fig. 8A, B). It was reported that downregulation of ICAM-1 at the mRNA and protein levels led to a strong suppression of human breast cancer cell invasion [40] and that subconjunctival injection of an anti-ICAM-1 (CD54) antibody produced a significant reduction in the growth of intraocular melanomas [41]. Further study will be needed to clarify how ICAM-1 molecules are involved in the process of higher migration and anchorage-independent growth.

Several studies indicate that CD43 (sialophorin), a highly glycosylated transmembrane protein, directly involved in cell-cell interaction [42]. The binding of CD43 to ICAM-1 has been demonstrated [43]. Moreover, CD43 has been shown to play a role in tumor-peritoneal adhesion [44] and to increase cell growth and colony formation in mouse and human cells [45]. Thus, CD43 may be one of the candidates of the ligand to ICAM-1. Further studies will be of significance to determine the ligand of ICAM-1 in our model.

In conclusion, our newly established, highly metastatic 4T1E/M3 cell line may serve as a potentially powerful new tool to study the mechanisms underlying bone marrow metastasis and to develop novel therapeutic strategies for treating metastatic breast cancer. The function of other upregulated and downregulated gene expression in tumor growth and metastasis in this model are the subjects of ongoing studies in our laboratory.

Acknowledgements We thank Ms. Yoko Ezaki for her excellent technical assistance for cell culture, Dr. Toru Imamura at AIST for making his laboratory facilities available for this study. This work was financially supported by Talent in Nanobiotechnology Course, Promotion Budget for Science and Technology from Ministry of Education, Culture, Sports, Science and Technology (MEXT) and by Japan Science and Technology Agency (JST).

References

1. Mundy GR (2002) Metastasis to bone: causes, consequences and therapeutic opportunities. Nat Rev Cancer 2:584–593
2. Parkin DM, Bray F, Ferlay J et al (2005) Global cancer statistics, 2002. CA Cancer J Clin 55:74–108
3. Bellahcene A, Bachelier R, Detry C et al (2007) Transcriptome analysis reveals an osteoblast-like phenotype for human osteotropic breast cancer cells. Breast Cancer Res Treat 101:135–148
4. Peyruchaud O, Winding B, Pecheur I et al (2001) Early detection of bone metastases in a murine model using fluorescent human breast cancer cells: application to the use of the bisphosphonate zoledronic acid in the treatment of osteolytic lesions. J Bone Miner Res 16:2027–2034
5. Yoneda T, Williams PJ, Hiraga T et al (2001) A bone-seeking clone exhibits different biological properties from the MDA-MB-231 parental human breast cancer cells and a brain-seeking clone in vivo and in vitro. J Bone Miner Res 16:1486–1495
6. Bandyopadhyay A, Elkahloun A, Baysa SJ et al (2005) Development and gene expression profiling of a metastatic variant of the human breast cancer MDA-MB-435 cells. Cancer Biol Ther 4:168–174
7. Bandyopadhyay A, Agyin JK, Wang L et al (2006) Inhibition of pulmonary and skeletal metastasis by a transforming growth factor-beta type I receptor kinase inhibitor. Cancer Res 66:6714–6721
8. Sheridan C, Kishimoto H, Fuchs RK et al (2006) CD44+/CD24- breast cancer cells exhibit enhanced invasive properties: an early step necessary for metastasis. Breast Cancer Res 8:R59
9. Liotta LA, Kohn EC (2001) The microenvironment of the tumour-host interface. Nature 411:375–379
10. Luo Y, Zhou H, Krueger J et al (2006) Targeting tumor-associated macrophages as a novel strategy against breast cancer. J Clin Invest 116:2132–2141
11. Condeelis J, Pollard JW (2006) Macrophages: obligate partners for tumor cell migration, invasion, and metastasis. Cell 124:263–266
12. Aslakson CJ, Miller FR (1992) Selective events in the metastatic process defined by analysis of the sequential dissemination of subpopulations of a mouse mammary tumor. Cancer Res 52:1399–1405
13. Pulaski BA, Ostrand-Rosenberg S (1998) Reduction of established spontaneous mammary carcinoma metastases following immunotherapy with major histocompatibility complex class II and B7.1 cell-based tumor vaccines. Cancer Res 58:1486–1493
14. Pulaski BA, Terman DS, Khan S et al (2000) Cooperativity of Staphylococcal aureus enterotoxin B superantigen, major histocompatibility complex class II, and CD80 for immunotherapy of advanced spontaneous metastases in a clinically relevant postoperative mouse breast cancer model. Cancer Res 60:2710–2715
15. Monzavi-Karbassi B, Artaud C, Jousheghany F et al (2005) Reduction of spontaneous metastases through induction of carbohydrate cross-reactive apoptotic antibodies. J Immunol 174:7057–7065
16. Lewis JD, Shearer MH, Kennedy RC et al (2005) Surrogate tumor antigen vaccination induces tumor-specific immunity and the rejection of spontaneous metastases. Cancer Res 65:2938–2946
17. Demaria S, Kawashima N, Yang AM et al (2005) Immune-mediated inhibition of metastases after treatment with local radiation and CTLA-4 blockade in a mouse model of breast cancer. Clin Cancer Res 11:728–734
18. Brilliant MH, Gondo Y, Eicher EM (1991) Direct molecular identification of the mouse pink-eyed unstable mutation by genome scanning. Science 252:566–569
19. Tominaga H, Ishiyama M, Ohseto F et al (1999) A Water-soluble tetrazolium salt useful for colorimetric cell viability assay. Anal Commun 36:47–50
20. Carmichael J, DeGraff WG, Gazdar AF et al (1987) Evaluation of a tetrazolium-based semiautomated colorimetric assay: assessment of chemosensitivity testing. Cancer Res 47:936–942
21. Okada T, Li J, Kodaka M et al (1998) Enhancement of type IV collagenases by highly metastatic variants of HT1080 fibrosarcoma cells established by a transendothelial invasion system in vitro. Clin Exp Metastasis 16:267–274
22. Palmieri D, Halverson DO, Ouatas T et al (2005) Medroxyprogesterone acetate elevation of Nm23-H1 metastasis suppressor expression in hormone receptor-negative breast cancer. J Natl Cancer Inst 97:632–642
23. Okada T, Akikusa S, Okuno H et al (2003) Bone marrow metastatic myeloma cells promote osteoclastogenesis through RANKL on endothelial cells. Clin Exp Metastasis 20:639–646
24. Ohta H, Hamada J-I, Tada M et al (2006) HOXD3-overexpression increases integrin $\alpha v\beta 3$ expression and deprives E-cadherin while it enhances cell motility in A549 cells. Clin Exp Metastasis 23:381–390
25. Coleman RE (2006) Clinical features of metastatic bone disease and risk of skeletal morbidity. Clin Cancer Res 12:6243s–6249s

26. Pulaski BA, Clements VK, Pipeling MR et al (2000) Immunotherapy with vaccines combining MHC class II/CD80+ tumor cells with interleukin-12 reduces established metastatic disease and stimulates immune effectors and monokine induced by interferon gamma. Cancer Immunol Immunother 49:34–45
27. Minn AJ, Gupta GP, Siegel PM et al (2005) Genes that mediate breast cancer metastasis to lung. Nature 436:518–524
28. Waghorne C, Thomas M, Lagarde A et al (1988) Genetic evidence for progressive selection and overgrowth of primary tumors by metastatic cell subpopulations. Cancer Res 48:6109–6114
29. Frost P, Kerbel RS, Hunt B et al (1987) Selection of metastatic variants with identifiable karyotypic changes from a nonmetastatic murine tumor after treatment with 2′-deoxy-5-azacytidine or hydroxyurea: implications for the mechanisms of tumor progression. Cancer Res 47:2690–2695
30. Eckhardt BL, Parker BS, van Laar RK et al (2005) Genomic analysis of a spontaneous model of breast cancer metastasis to bone reveals a role for the extracellular matrix. Mol Cancer Res 3:1–13
31. Irshad S, Pedley RB, Anderson J et al (2004) The Brn-3β transcription factor regulates the growth, behavior, and invasiveness of human neuroblastoma cells in vitro and in vivo. J Biol Chem 279:21617–21627
32. Lee JY, Kim H, Ryu CH et al (2004) Merlin, a tumor suppressor, interacts with transactivation-responsive RNA-binding protein and inhibits its oncogenic activity. J Biol Chem 279:30265–30273
33. Muraoka-Cook RS, Kurokawa H, Koh Y et al (2004) Conditional overexpression of active transforming growth factor beta1 in vivo accelerates metastases of transgenic mammary tumors. Cancer Res 64:9002–9011
34. Glondu M, Liaudet-Coopman E, Derocq D et al (2002) Down-regulation of cathepsin-D expression by antisense gene transfer inhibits tumor growth and experimental lung metastasis of human breast cancer cells. Oncogene 21:5127–5134
35. Morimoto-Tomita M, Ohashi Y, Matsubara A et al (2005) Mouse colon carcinoma cells established for high incidence of experimental hepatic metastasis exhibit accelerated and anchorage-independent growth. Clin Exp Metastasis 22:513–521
36. Gupta GP, Massague J (2006) Cancer metastasis: building a framework. Cell 127:679–695
37. Hu J, Verkman AS (2006) Increased migration and metastatic potential of tumor cells expressing aquaporin water channels. FASEB J 20:1892–1894
38. Chen X, Lin J, Kanekura T et al (2006) A small interfering CD147-targeting RNA inhibited the proliferation, invasiveness, and metastatic activity of malignant melanoma. Cancer Res 66:11323–11330
39. Galaup A, Cazes A, Le Jan S et al (2006) Angiopoietin-like 4 prevents metastasis through inhibition of vascular permeability and tumor cell motility and invasiveness. Proc Natl Acad Sci USA 103:18721–18726
40. Rosette C, Roth RB, Oeth P et al (2005) Role of ICAM1 in invasion of human breast cancer cells. Carcinogenesis 26:943–950
41. Wang S, Coleman EJ, Pop LM et al (2006) Effect of an anti-CD54 (ICAM-1) monoclonal antibody (UV3) on the growth of human uveal melanoma cells transplanted heterotopically and orthotopically in SCID mice. Int J Cancer 118:932–941
42. Fanales-Belasio E, Zambruno G, Cavani A, Girolomoni G (1997) Antibodies against sialophorin (CD43) enhance the capacity of dendritic cells to cluster and activate T lymphocytes. J Immunol 159:2203–2211
43. Rosenstein Y, Park JK, Hahn WC et al (1991) CD43, a molecule defective in Wiskott-Aldrich syndrome, binds ICAM-1. Nature 354:233–235
44. Ziprin P, Alkhamesi NA, Ridgway PF, Pech DH, Darzi AW (2004) Tumor-expressed CD43 (sialophorin) mediates tumour-mesothelial cell adhesion. Biol Chem 385:755–761
45. Kadaja-Saarepuu L, Laos S, Jããger K et al (2007) CD43 promotes cell growth and helps to evade FAS-mediated apoptosis in non-hematopoietic cancer cell lacking the tumor suppressors p53 or ARF. Oncogene (advance online publication). doi: 10.1038/sj.onc.1210802